New insights on thermal properties of asteroids using IR interferometry

Alexis MATTER — Max-Planck-Institut für Radioastronomie

Marco Delbo — Observatoire de la CÔTE d'AZUR

Benoit Carry — esa

Sebastiano Ligori — INAF ISTITUTO NAZIONALE DI ASTROFISICA NATIONAL INSTITUTE FOR ASTROPHYSICS

Madrid, March 8th 2012

PLAN

Introduction

Thermal properties of asteroids

- Physical parameters
- Physical information
- Scientific interest

Interferometry

Thermophysical modeling

- Principle
- Application : Main-belt asteroids (41) Daphne and (16) Psyche

Conclusion and perspectives

Introduction

Introduction

Asteroids and the origin of our solar system

- Asteroids → debris of the planet formation process
- Small → little alteration →conserve pristine material
- Asteroids suffered collisional evolution
- Sizes, shapes, bulk densities, surface properties → collisional evolution

Introduction

Main-belt asteroids

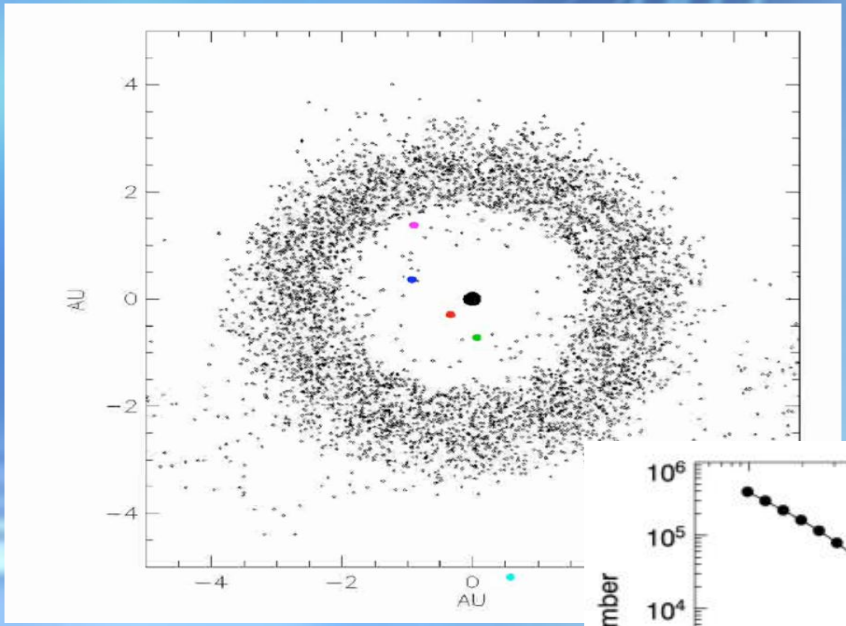

Plot of the positions of the first 5000 asteroids

Size distribution

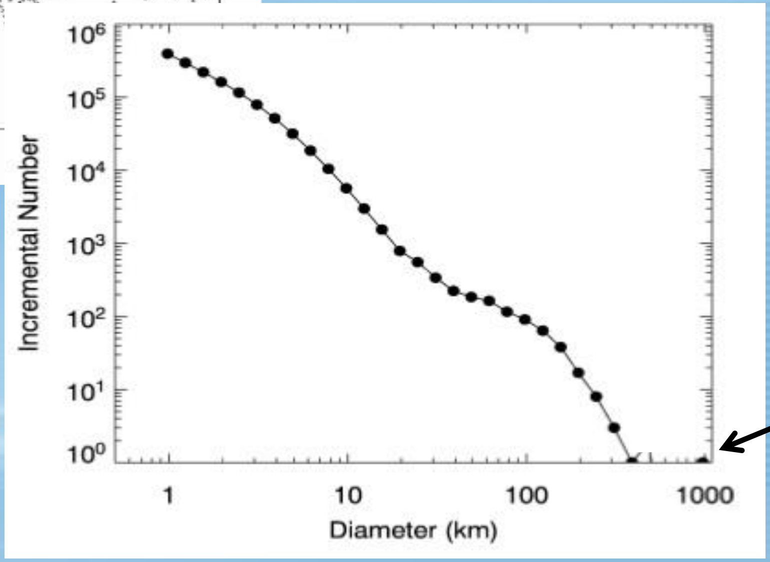

Bottke et al. (2005)

(1) Ceres

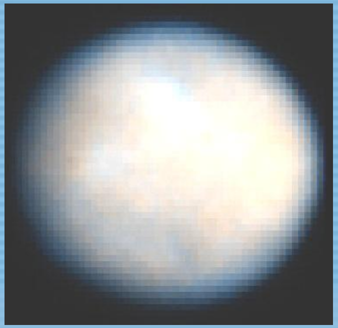

980 km

Near-Earth asteroids (NEAs)

Location

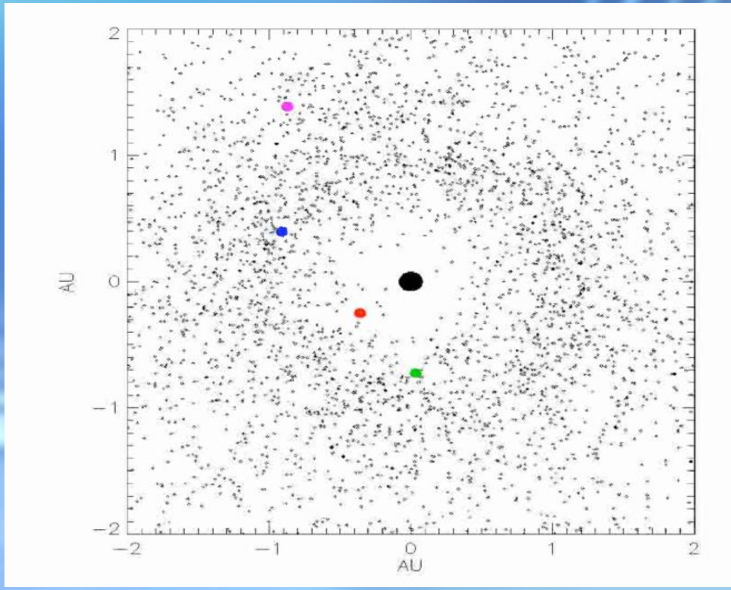

Size distribution

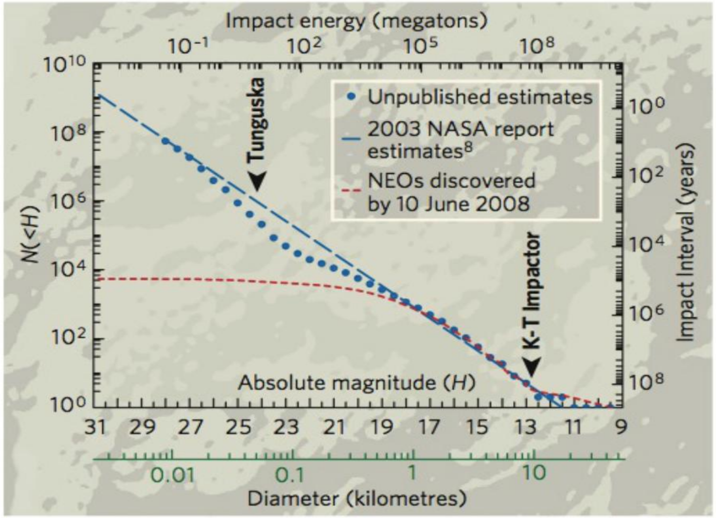

Figure 1 | Estimate of the cumulative population of near-Earth objects (NEOs) versus size. *H* is the absolute magnitude

Origin :
- Some are from the main belt
- Some are dead comets

Doom :
- Crash into the Sun
- Ejection out of the solar system
- Impact on a planet

Thermal properties of asteroids

Thermal properties of asteroids : physical parameters

Thermal inertia

- Measure of the resistance of a material to a temperature change
- $\Gamma = \sqrt{\rho \kappa c}$ in SI units: $J.m^{-2}.s^{-0.5}.K^{-1}$
  - ρ: **Density**
  - κ: **Thermal conductivity**
  - c: **Specific heat**

Surface roughness

- Surface parameter impacting the beaming effect
- Modeled by adding hemispherical craters

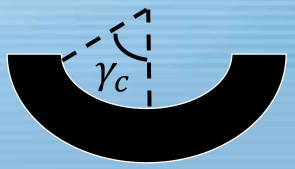

crater

γ_c : Opening angle

ρ_c : Crater density

Thermal properties of asteroids : physical parameters

Effect on thermal emission

Thermal inertia

Smoothing of the surface temperature distribution

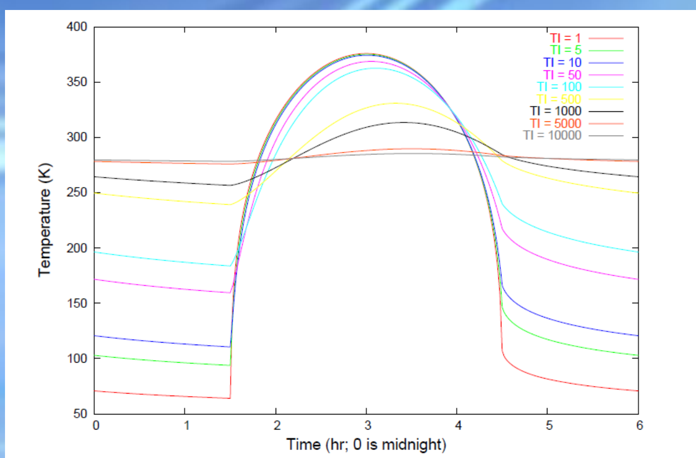

Mueller (2004)

Midnight

Noon (insolation peak)

Surface roughness

Increase of the apparent temperature when surface is viewed at a small solar phase angle (thermal emission 'beamed' in the sunward direction)

Opposition effect in the visible (Eugene Cernan on the moon)

Credits : Michael Light

The opposition effect brightens the area around Eugene Cernan''s shadow due to retroreflective properties of lunar regolith.

Thermal properties of asteroids : physical information

Thermal inertia → Presence (or absence), depth and thickness of regolith, and presence of exposed rocks on the surface of atmosphere–less bodies

(25143) Itokawa	(433) Eros	The Moon	(21) Lutetia
$\Gamma = 750$	$\Gamma = 150$	$\Gamma = 50$	$\Gamma = 20$
	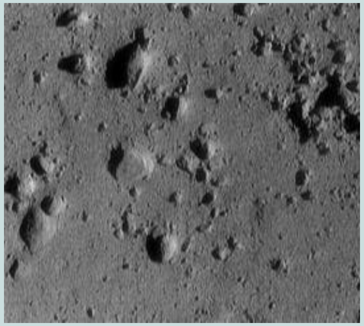	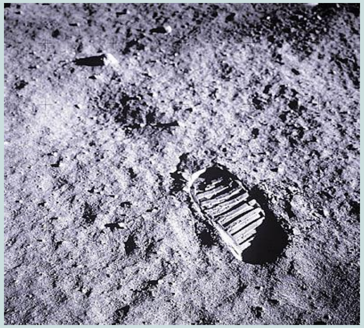	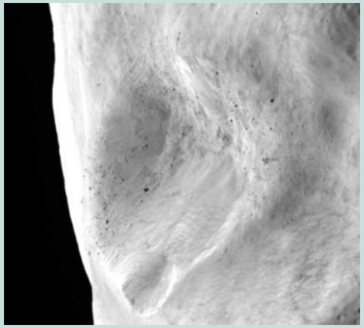
Coarse regolith and boulders	Finer and thicker regolith	Mature and fine regolith	Very fine regolith

Thermal properties of asteroids : correlation with size

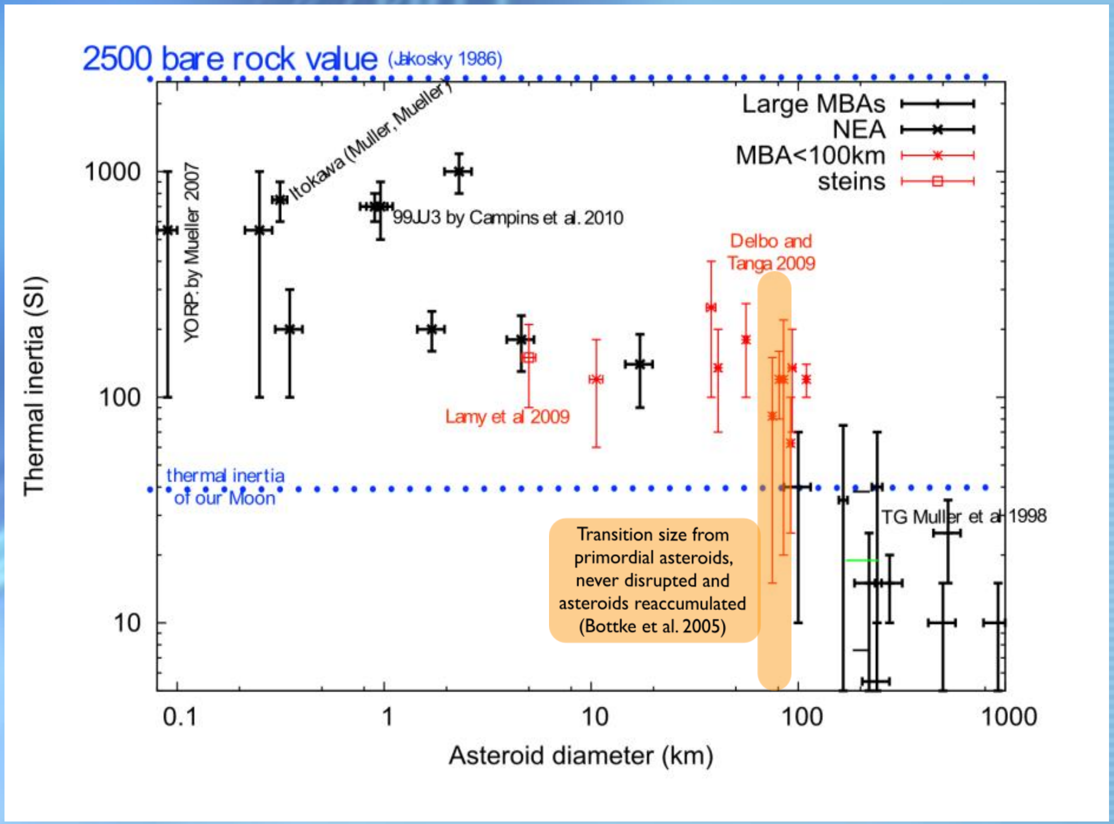

Inverse correlation size-thermal inertia

$\Gamma \propto D^{-\xi}$

ξ_{small} — NEAs and MBAs with D ≤ 80-100 km

ξ_{big} — MBAs with D ≥ 80-100 km

Thermal properties of asteroids : Scientific interest

Strenght of the Yarkovsky effect

Binzel et al. (2003)

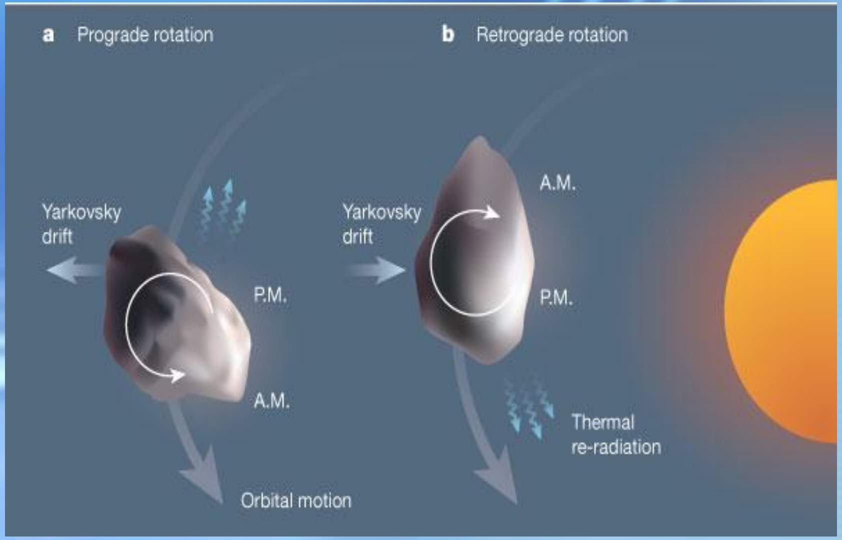

Semi-major axis drift rate

$\Gamma = cte$ with D $\rightarrow$ $\frac{da}{dt} \propto D^{-1}$ **Bottke et al. (2002)**

Semi-major axis drift rate

$\Gamma \propto D^{-\xi}$ $\rightarrow$ $\frac{da}{dt} \propto D^{\xi-1}$ **Delbo&Tanga (2009)**

Size distribution of asteroids injected into the Near-Earth space is modified

Thermal inertia → impact prediction for hazardous asteroids

Thermal properties of asteroids : Scientific interest

Refinement of size measurements

IR radiometry -> 140000 asteroids measured from simple thermal modeling of IR emission (See **Mazieros et al. (2011)**)

IR flux

$I(\lambda)$ →

Thermal model
(spherical shape, zero thermal inertia)

→ **Albedo size**

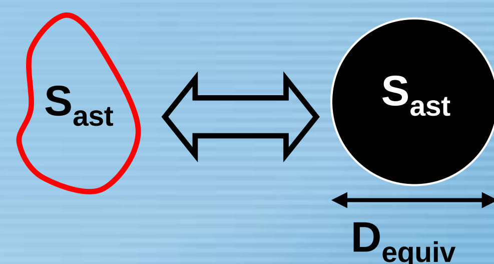

STM
Standard Thermal Model (Lebovski et al., 1986)

If non-negligible thermal inertia → Diameter underestimation / Albedo overestimation

Spencer et al. (1989)

Infrared Interferometry

IR interferometry : principle

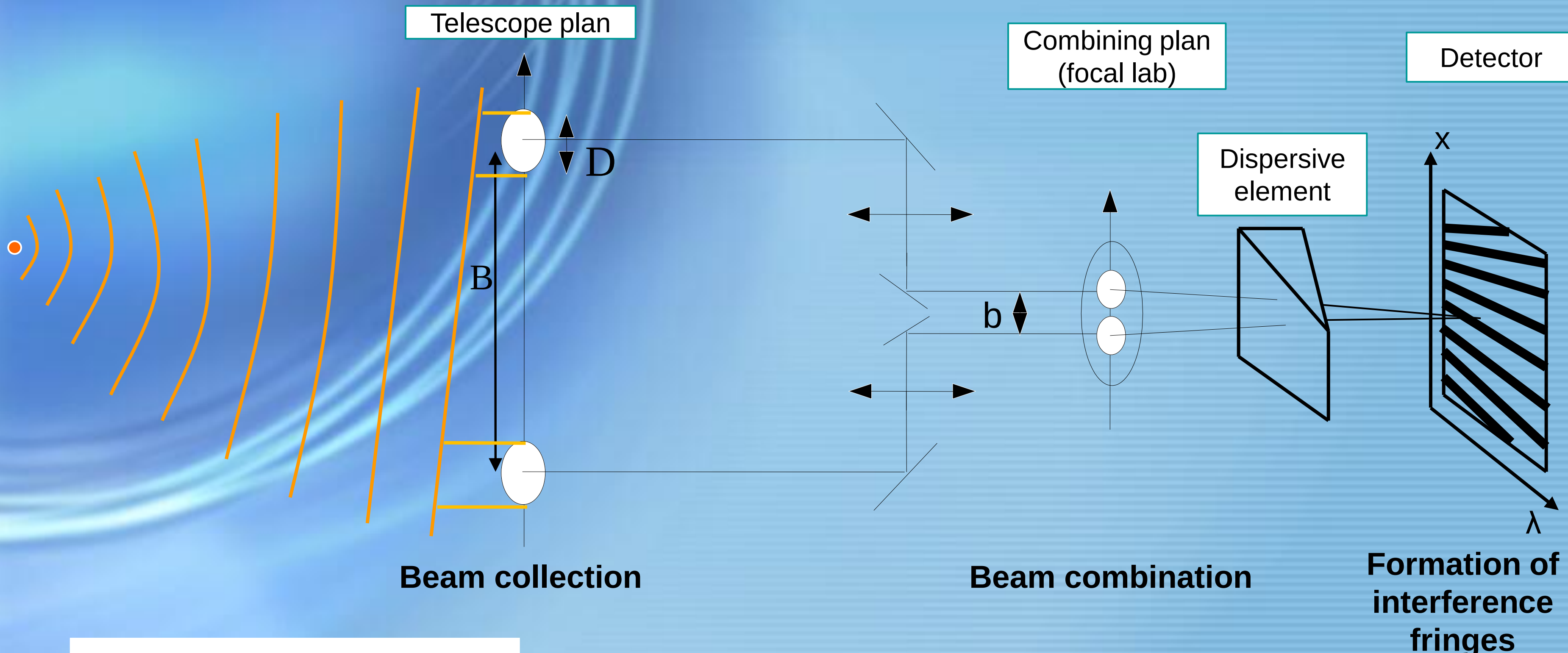

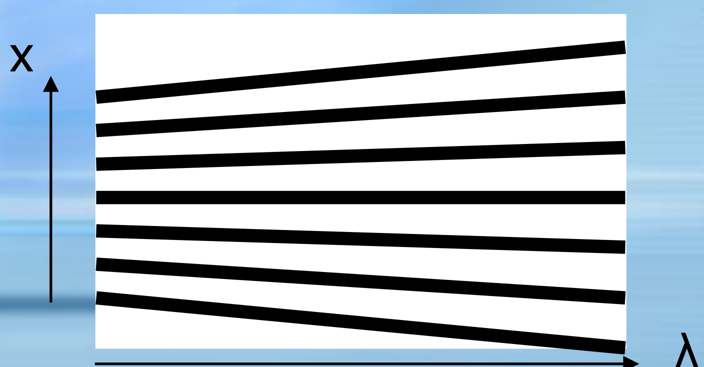

$$I(x,\lambda) = I_0[1+\cos(a\frac{x}{\lambda})]$$

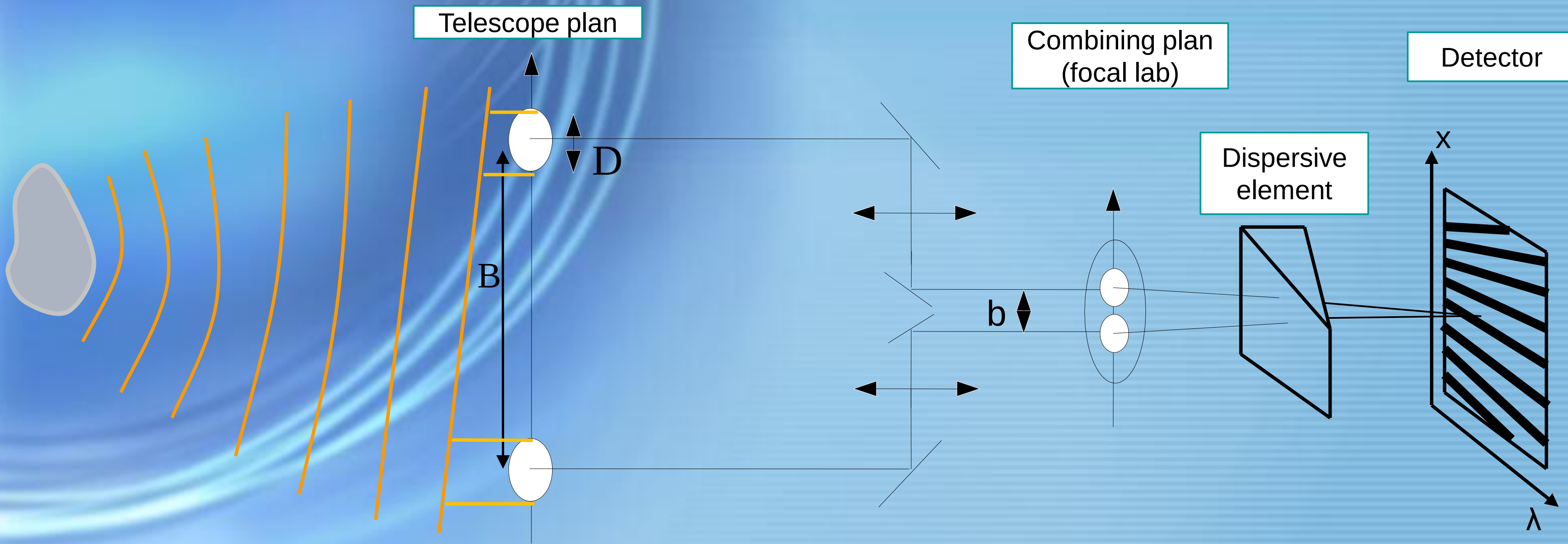

Beam collection

Beam combination

Formation of interference fringes

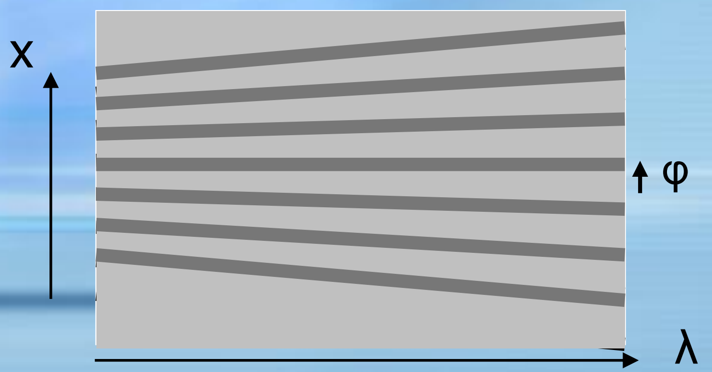

$$I(x,\lambda)=I_0[1+C(\tfrac{B}{\lambda}).\cos(a\frac{x}{\lambda}+\varphi(\tfrac{B}{\lambda}))]$$

Fringes contrast (visibility) → V(λ)

Fringes phase → φ(λ)

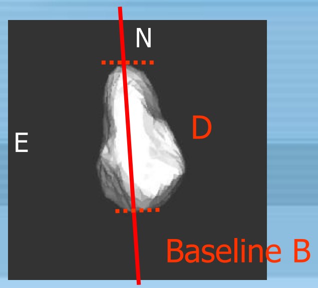

IR interferometry : instrumentation

ESO VLTI

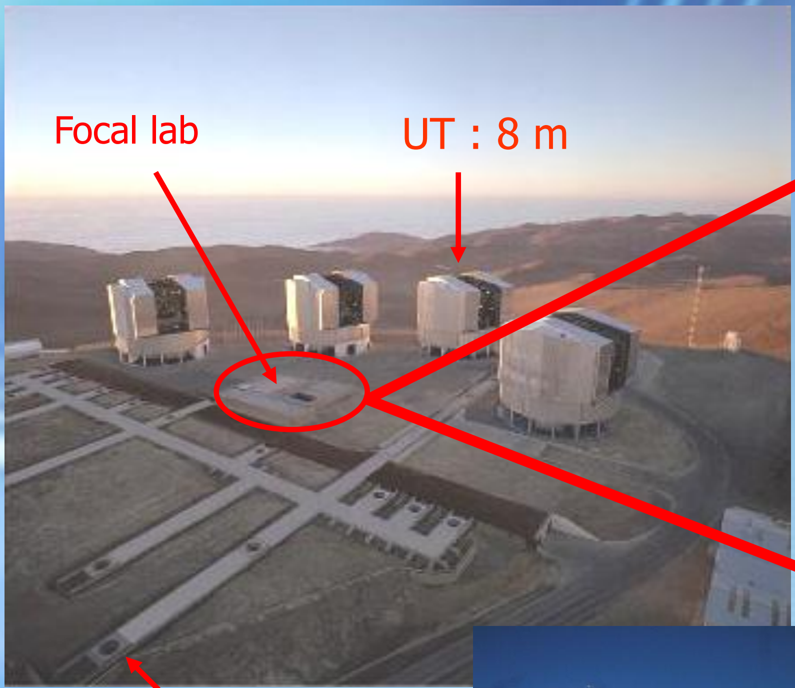

AT : 1.8 m

AMBER
3 telescopes

$\lambda \in [1.2 - 2.5]\mu m$

$\theta \sim \frac{B}{\lambda} \in [3 - 25] mas$

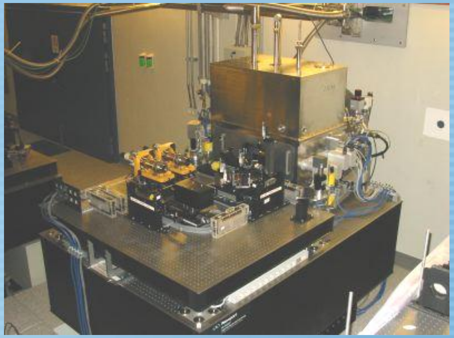

MIDI
2 télescopes

$\lambda \in [8 - 13]\mu m$

$\theta \sim \frac{B}{\lambda} \in [15 - 100] mas$

Sensitive enough for observation of MBAs (T ~ 250-300 K)

Thermophysical modeling

Thermophysical modeling: principle

Shape model
- distances
- rotation axis
- shape and size

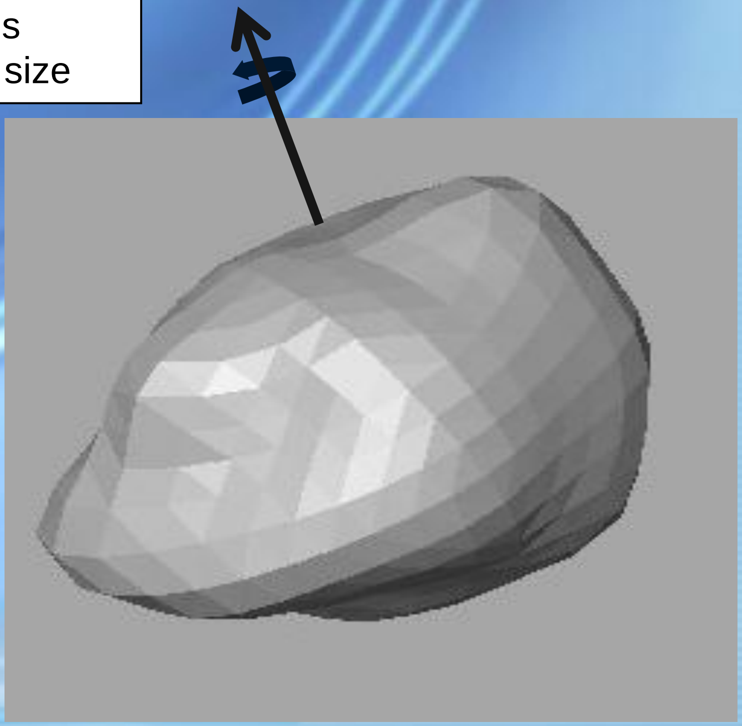

Input

TPM

Thermophysical modeling: principle

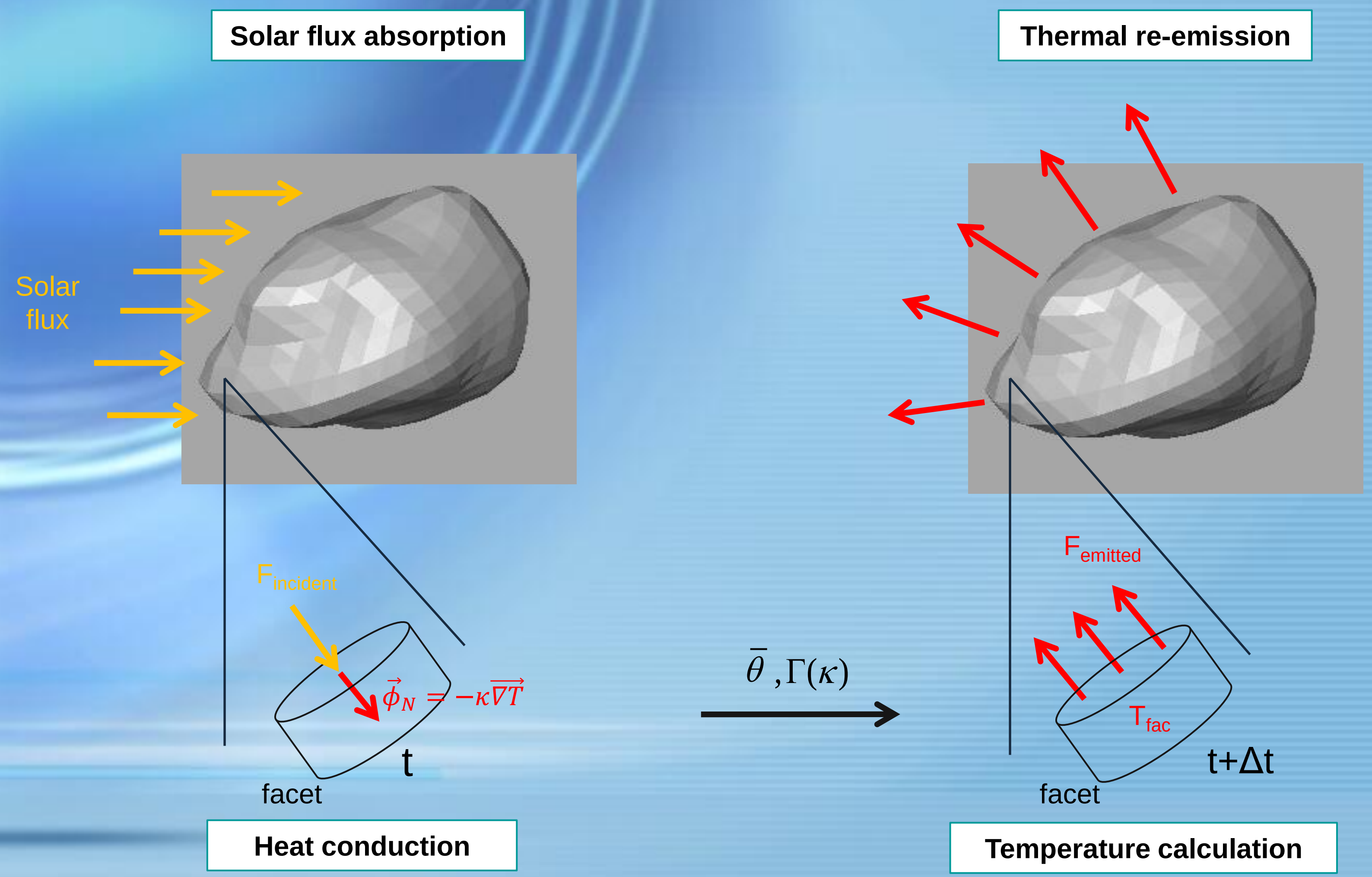

Thermophysical modeling: principle

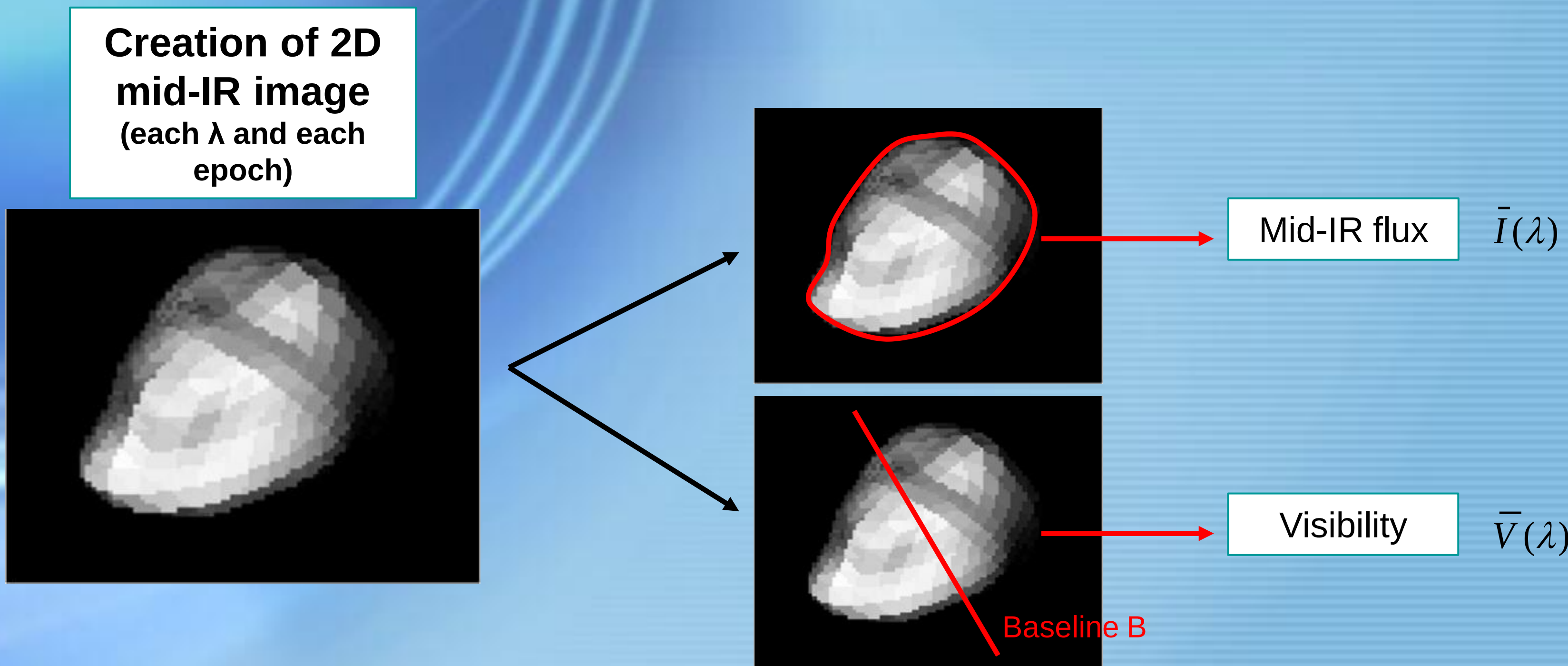

Thermophysical modeling: principle

χ^2 calculation

roughness model

Γ value

Observations

$V(\lambda)$ et $I(\lambda)$

$\bar{V}(\lambda)$ et $\bar{I}(\lambda)$

Model

$$\chi_{i,j}^{\;2} = \left[\frac{I_i(\lambda_j) - \bar{I}_i(\lambda_j)}{\sigma_{I_{i,j}}}\right]^2 + \left[\frac{V_i(\lambda_j) - \bar{V}_i(\lambda_j)}{\sigma_{V_{i,j}}}\right]^2$$

observing epoch (i) — **wavelength** (j)

$$\chi^2 = \frac{1}{N_e N_l} \sum_i \sum_j \chi_{i,j}^{\;2}$$

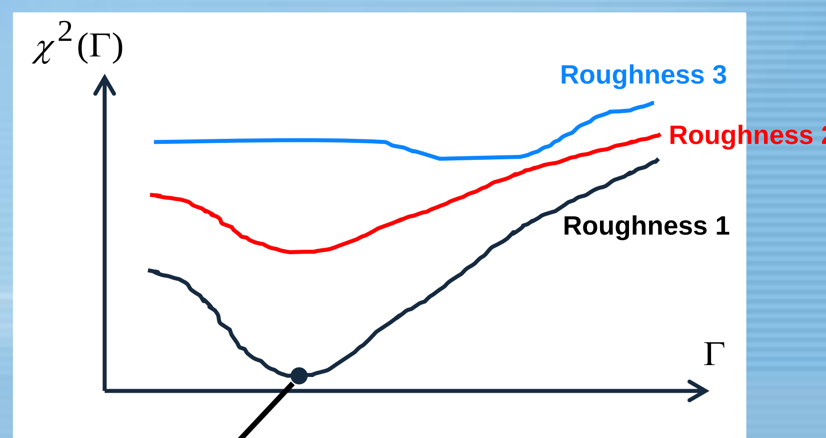

Best-fit value for roughness model, thermal inertia, albedo, size

Thermophysical modeling: interest of interferometry

$I(\lambda) \propto D_{proj}{}^2$

$V(\lambda) = f(D_{ang})$

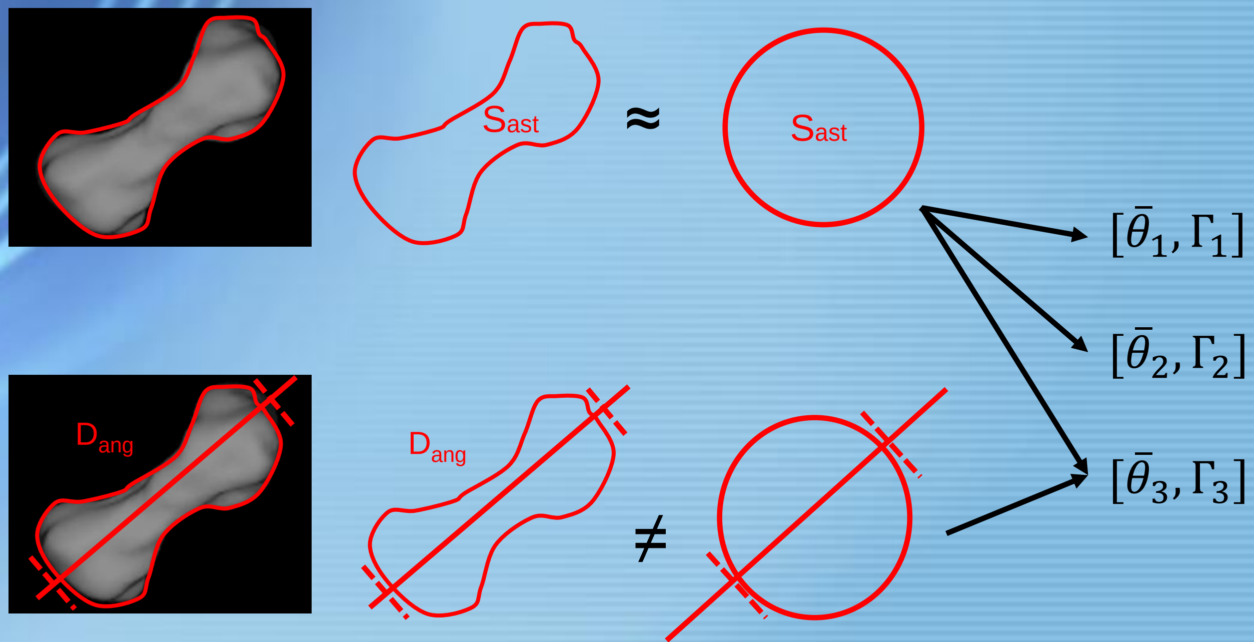

At one single epoch, flux + visibility → strong constraint on thermal properties

Thermophysical modeling : (41) Daphne

(41) Daphne

Big main-belt asteroid (D ~ 220 km)

Spectral properties (albedo) → **C-type asteroid** ↔ primitive carbonaceous chondrite meteorites

Lightcurves observations and disk-resolved observations

Shape model →

Non-convex model (Carry, 2009)

Observing campaign performed in March 2008 with ATs (baseline = 16m) (four mid-IR visibility and flux measurements)

Thermophysical modeling : (41) Daphne

Shape model at the time of VLTI observations

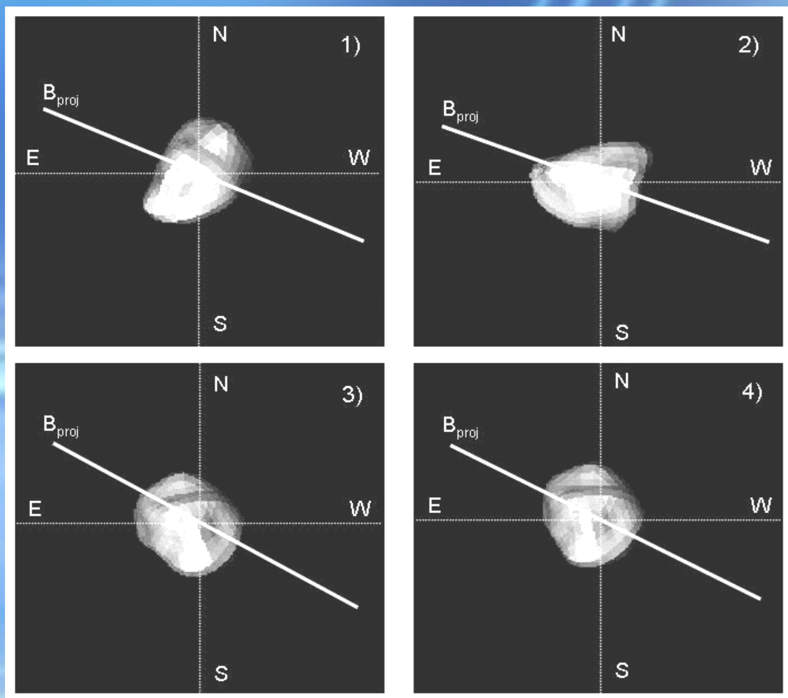

MIDI measurements + best-fit model

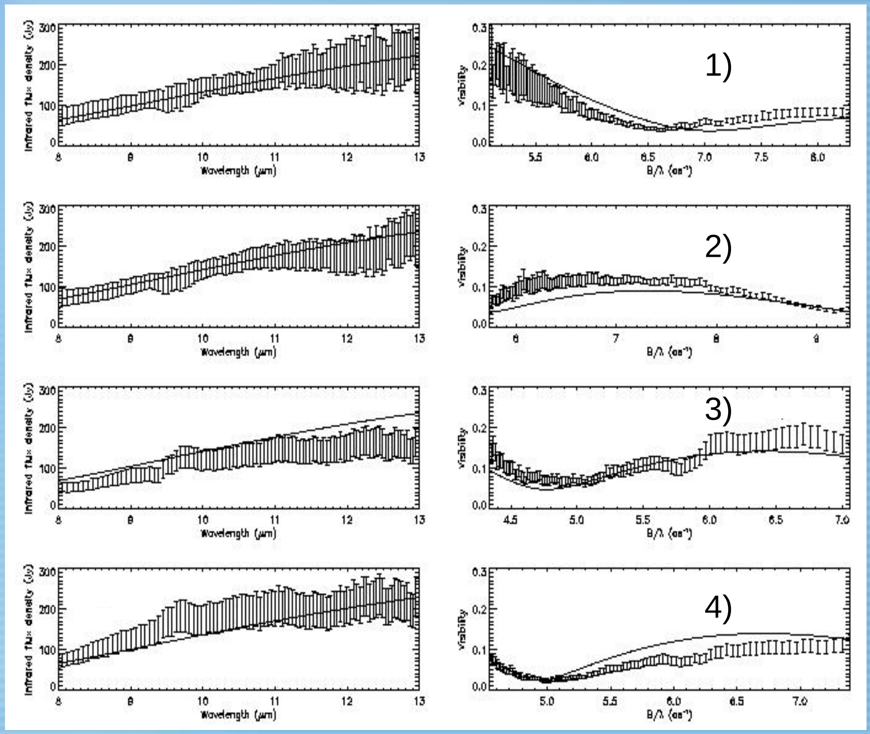

Mid-IR Visibility + Flux → TPM

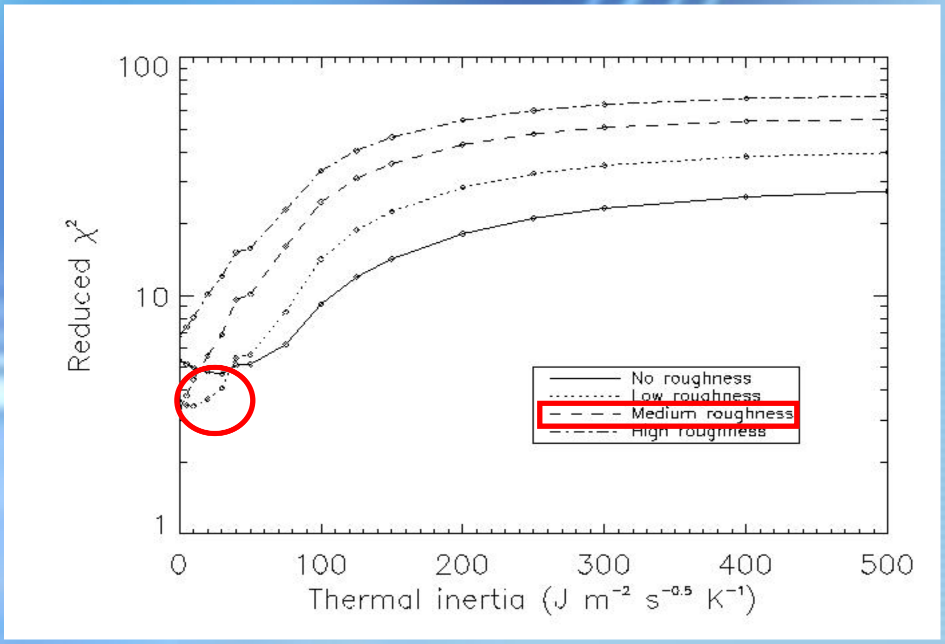

Moderate roughness $45^\circ \leq \gamma_c \leq 68^\circ$

$0.5 \leq \rho_c \leq 0.8$

(Moon and (1) Ceres → high roughness)

Γ< 30 J.m^{-2}.s^{-1}.K → very fine regolith

(Moon ≈ 50 J.m^{-2}.s^{-1}.K and (1) Cérès ≈ 15 J.m^{-2}.s^{-1}.K)

Thermophysical modeling : (41) Daphne

Mid-IR Visibility + Flux → TPM

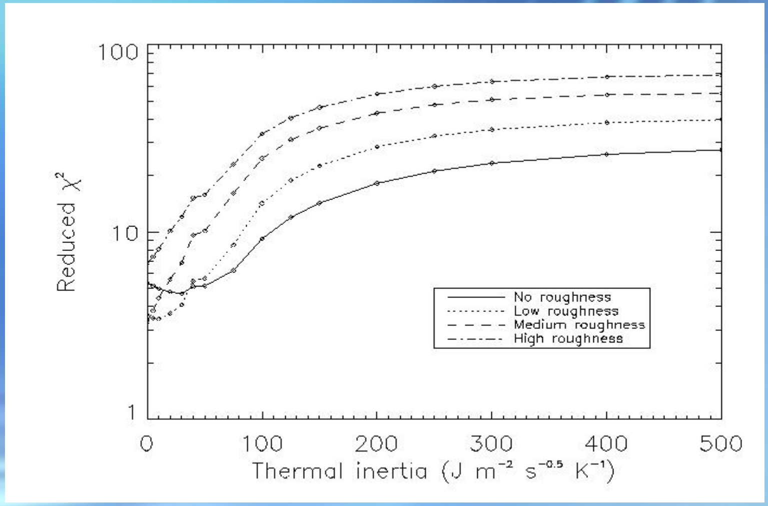

Mid-IR Flux → TPM

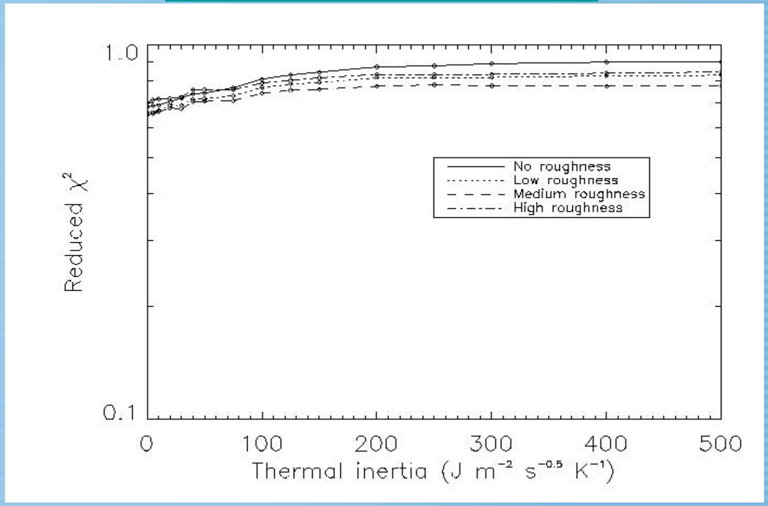

↓

Strong constraints brought by IR interferometry

Matter et al., 2011, ‘*Determination of physical properties of the asteroid (41) Daphne from interferometric observations in the thermal infrared*’, **Icarus**

(16) Psyche

Main-belt asteroid

Visible and near-IR spectral properties (albedo) → **M-type asteroid** ↔ Ni-Fe or stony-iron meteorites
(Hadersen et al., 1995; Ockert-Bell et al., 2010)

Very high radar albedo → strong evidence for a metal-rich surface regolith (Shepard et al., 2010)

size estimates (~ 230-260 km)→ densities **≤ 3 g/cm³ (silicate-rich)** or densities **≥ 3.5 g/cm³ (metal-rich)**
(Baer et al., 2008; Drummond & Christou, 2008)

Is M-type (16) Psyche a dense metal-rich asteroid ?
Origin: fragment of a differentiated body iron core ?

Thermophysical modeling : (16) Psyche

Non-convex model (Carry, 2011)

Lightcurves observations

Disk-resolved observations

Shape model →

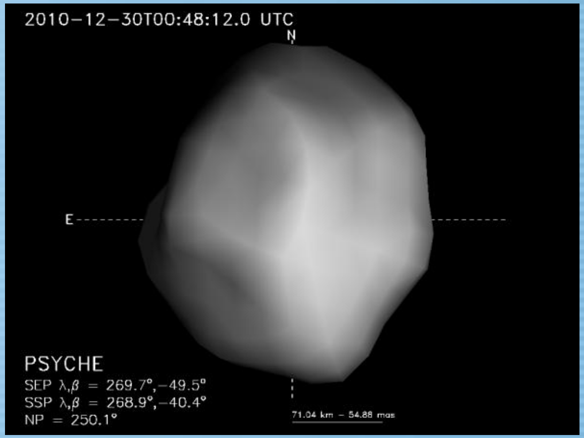

New observing campaign performed in December 2010 with ATs (baseline = 16m)
(five mid-IR visibility and flux measurements)

Thermophysical modeling : (16) Psyche

Shape model at the time of the VLTI observations

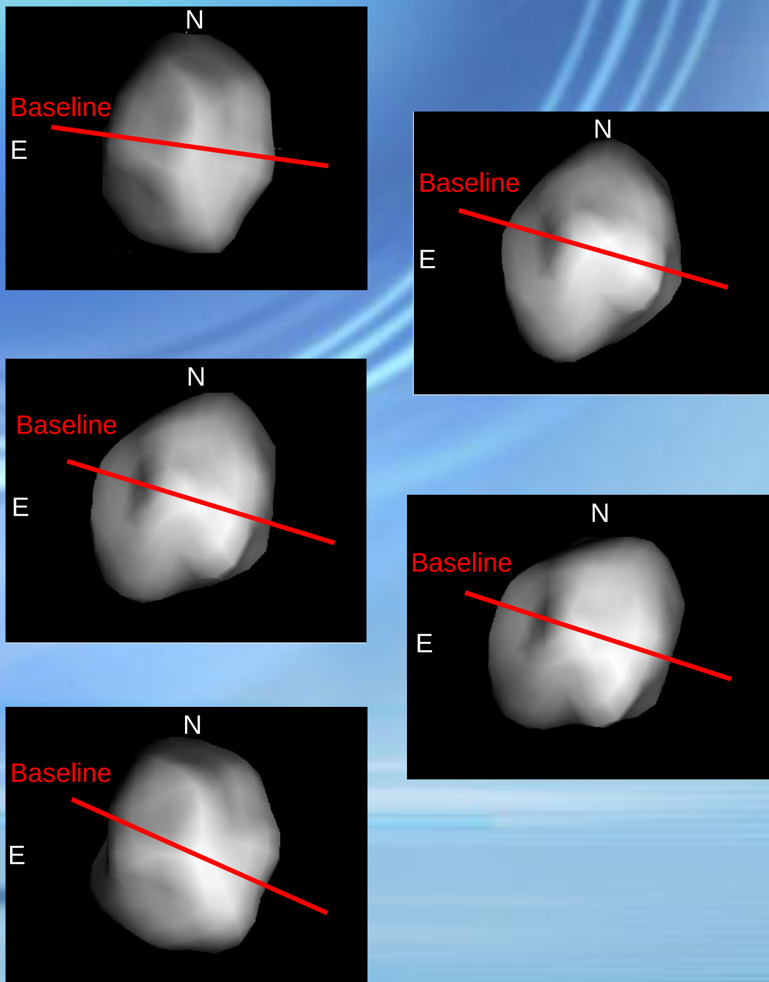

Visibilities and fluxes

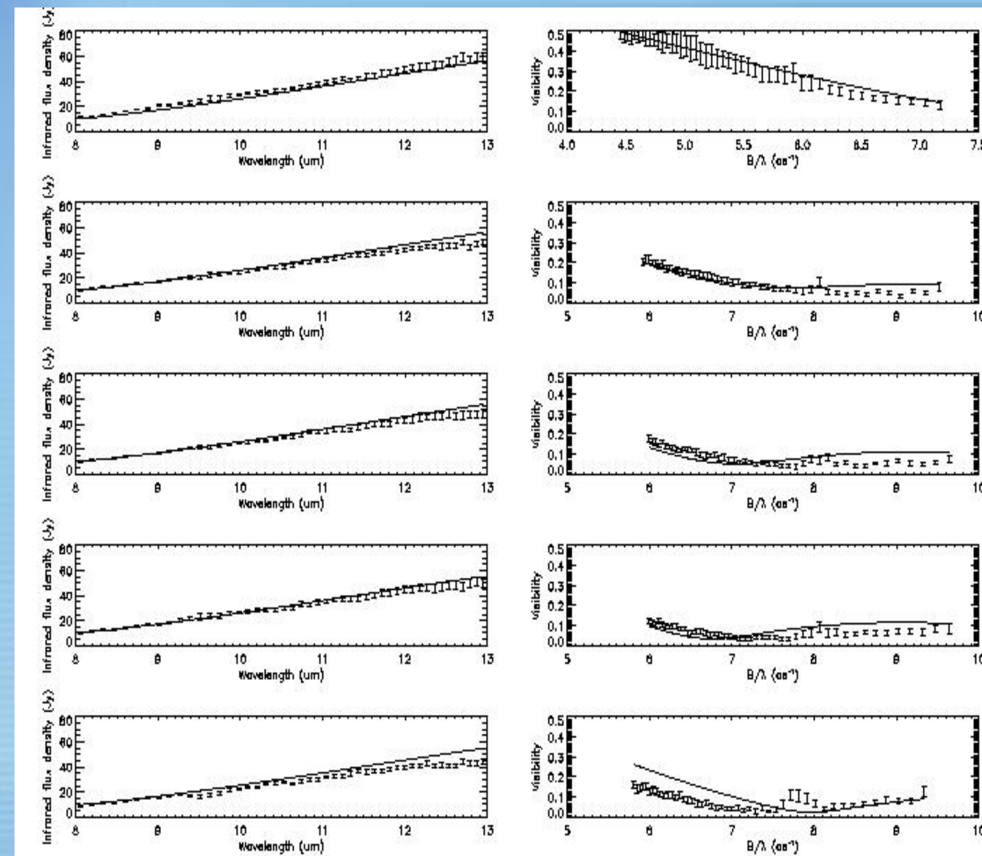

Thermophysical modeling : (16) Psyche

Mid-IR Visibility + Flux → TPM

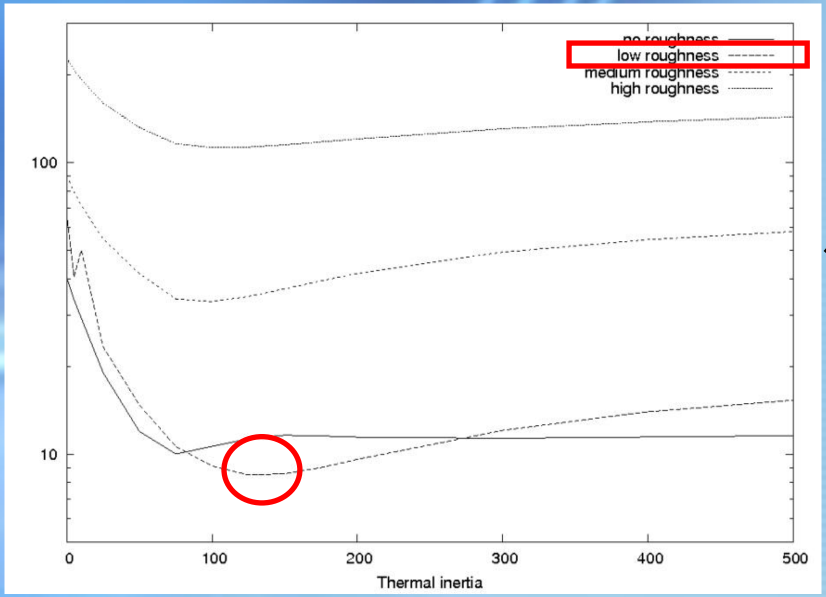

Low roughness

$$\gamma_c = 45^{\circ}$$

$$\rho_c = 0.5$$

Thermal inertia > 100 J.m^{-2}.s^{-1}.K

Volume equivalent diameter → ~ 235 km

Thermophysical modeling : (16) Psyche

First conclusions

Smaller diameter (~ 235 km)
→ density ≥ 3.5 g/cm^3

↓

Dense structure

High thermal inertia values (> 100 $J.m^{-2}.s^{-1}.K$)
→ little porosity of the surface

↓

High surface thermal conductivity

↘ ↙

Metal-rich regolith and internal structure

In progress : refinement of the shape model + use of complementary data

Thermophysical modeling : size vs thermal inertia

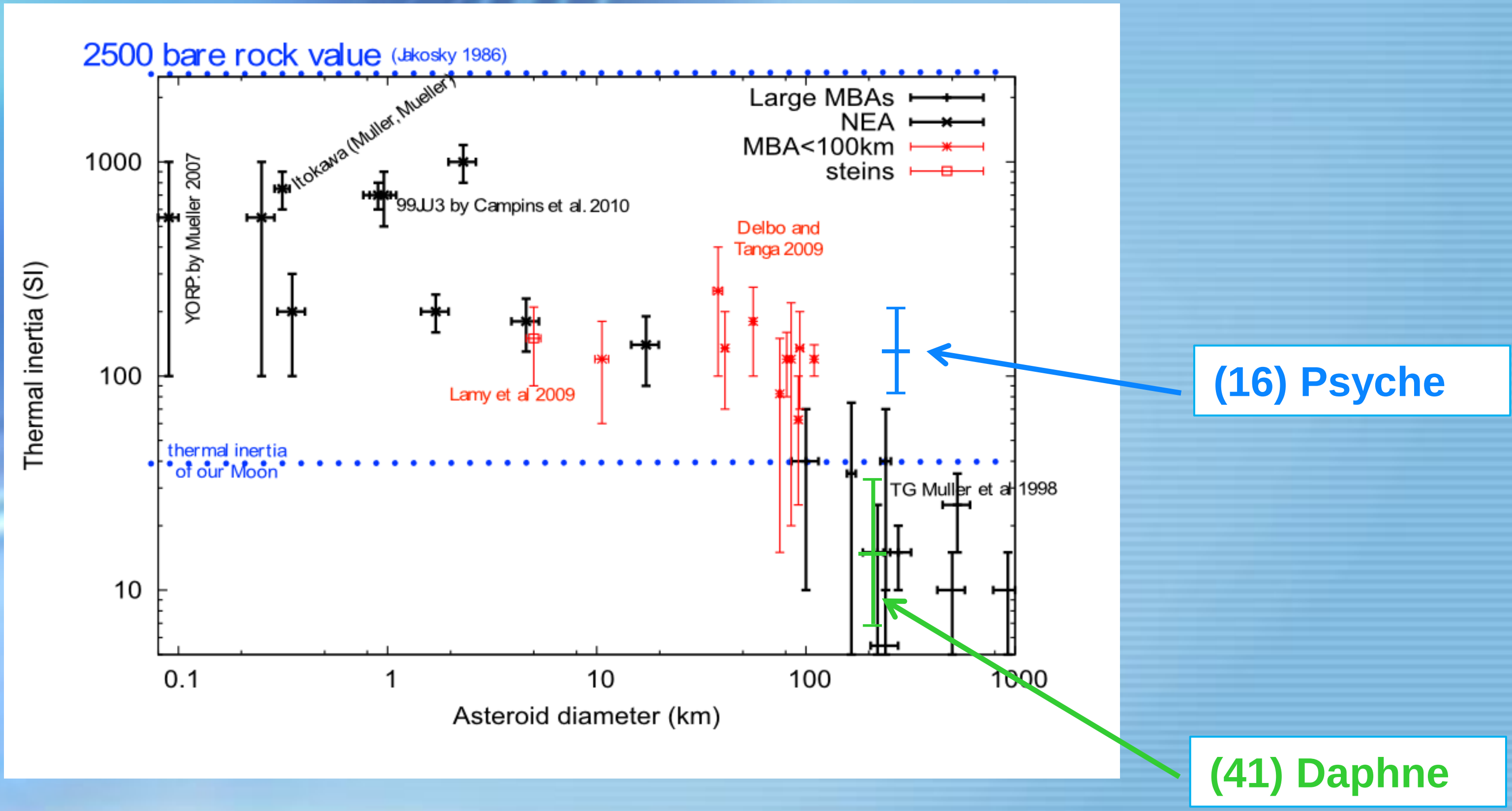

Conclusion and perspectives

Conclusion and perspectives

Summary

• First application of IR interferometry to the study of thermal properties of asteroids

→ (41) Daphne : **. First constraints on thermal inertia and surface roughness (Matter et al., 2011)**

→ (16) Psyche : **. Preliminary results on size and thermal inertia** → **metallic composition**

↳ **In progress**

Perspectives

↓

New VLTI instrument PRIMA

↓

Larger panel of asteroids observable with MIDI
(expected gain of about 3 magnitudes in V)

↙ ↘

Thermal properties **Internal structure**

Thank you for your attention

Madrid, March 8th 2012